Cellular/Molecular

The Antiseizure Drug Perampanel Is a Subunit-Selective Negative Allosteric Modulator of Kainate Receptors

Sakiko Taniguchi, Jacob R. Stolz, and Geoffrey T. Swanson
Department of Pharmacology, Northwestern University Feinberg School of Medicine, Chicago, Illinois 60611

Perampanel (PMP) is a third-generation antiseizure drug reported to be a potent and selective noncompetitive negative allosteric modulator of one subfamily of ionotropic glutamate receptor (iGluR), the α-amino-3-hydroxy-S-methylisoxazole-4-propionic acid receptors (AMPARs). However, the recent structural resolution of AMPARs in complex with PMP revealed that its binding pocket is formed from residues that are largely conserved in two members of another family of iGluRs, the GluK4 and GluK5 kainate receptor (KAR) subunits. We show here that PMP inhibits both recombinant and neuronal KARs, contrary to the previous reports, and that the negative allosteric modulator (NAM) activity requires GluK5 subunits to be channel constituents. PMP inhibited heteromeric GluK1/GluK5 and GluK2/GluK5 KARs at IC_{50} values comparable to that for AMPA receptors but was much less potent on homomeric GluK1 or GluK2 KARs. The auxiliary subunits Neto1 or Neto2 also made GluK2-containing KARs more sensitive to inhibition. Finally, PMP inhibited mouse neuronal KARs containing GluK5 subunits and Neto proteins in nociceptive dorsal root ganglia neurons and hippocampal mossy fiber–CA3 pyramidal neuron synapses. These data suggest that clinical actions of PMP could arise from differential inhibition of AMPAR or KAR signaling and that more selective drugs might maintain antiseizure efficacy while reducing adverse effects.

Key words: **anticonvulsant; electrophysiology; epilepsy; Fycompa; glutamate receptor; seizure**

Significance Statement

PMP is a regulatory approved antiseizure drug used for refractory partial-onset and generalized tonic-clonic seizures that acts as a selective negative allosteric modulator of AMPARs. Here, we demonstrate that PMP inhibits KARs, a second family of ionotropic glutamate receptors, in addition to AMPARs. NAM activity on KARs required GluK5 subunits or Neto auxiliary subunits as channel constituents. KAR inhibition, therefore, could contribute to PMP antiseizure action or the adverse effects that are significant with this drug. Drug discovery aimed at more selective allosteric modulators that discriminate between AMPARs and KARs could yield next-generation drugs with improved therapeutic profiles for treatment of epilepsy.

Introduction

Epilepsy is a common, chronic neurologic syndrome characterized by spontaneous recurrent seizures caused by hyperexcitability and synchronization in localized or diffuse brain circuits. Antiseizure drugs (ASDs) suppress the initiation and propagation of seizures through dampening neuronal excitability, reducing excitatory neurotransmission, or enhancing inhibitory tone (Sills and Rogawski, 2020). A significant fraction of patients, estimated at ~35%, remain refractory to seizure management with existing ASDs (Chen et al., 2018), highlighting the importance of identifying new drugs that preclude seizure generation and propagation (Golyala and Kwan, 2017). Perampanel (PMP; 2-(2-oxo-1-phenyl-5-pyridin-2-yl-1,2-dihydropyridin-3-yl)benzonitrile); Hanada et al., 2011) is a third-generation ASD that received regulatory approval in 2012 as an adjunct for refractory focal-onset seizures and treatment of generalized-onset tonic-clonic seizures. PMP also has mechanism-based adverse effects, however, that include dizziness, somnolence, ataxia, and psychiatric symptoms that occur in roughly the same dose range as its antiseizure activity (Zaccara et al., 2013; Rugg-Gunn, 2014; Zhuo et al., 2017; Villanueva et al., 2022).

The antiseizure activity of PMP is thought to arise through negative allosteric modulation of one subfamily of ionotropic glutamate receptors (iGluRs), the α-amino-3-hydroxy-5-methyl-isoxazole-4-propionic acid receptors (AMPARs; Hanada et al., 2011; Ceolin et al., 2012; Chen et al., 2014). AMPARs mediate fast excitatory neurotransmission in the central and peripheral nervous systems, and their inhibition by PMP dampens neuronal excitability and reduces synchronized firing of neural networks

Received Dec. 3, 2021; revised Apr. 27, 2022; accepted May 24, 2022.

Author contributions: S.T., J.R.S., and G.T.S. designed research; S.T., J.R.S., and G.T.S. performed research; S.T., J.R.S., and G.T.S. analyzed data; S.T. and G.T.S. wrote the paper.

This work was supported by grants from the National Institute of Neurological Disorders and Stroke to G.T.S. (R01NS105502 and R21NS123780)., and S.T. was supported by the Uehara Memorial Foundation. The authors thank Gil Shaulsky, Scott Myers, and Steve Traynelis (Emory University School of Medicine) for providing human *GRIK* clones.

The authors declare no competing financial interests.

Correspondence should be addressed to Geoffrey T. Swanson at gtswanson@northwestern.edu.

https://doi.org/10.1523/JNEUROSCI.2397-21.2022

(Rogawski, 2013). PMP has more favorable pharmacokinetic properties than other AMPAR-negative allosteric modulators (NAMs) such as talampanel (GYKI-53773; Zaccara et al., 2013; Patsalos, 2015), which in part could account for its successful development as an ASD (Rogawski, 2011).

PMP was reported to be a selective AMPAR NAM that did not inhibit NMDA or kainate receptors (KARs), the other two subfamilies of functional iGluRs (Hanada et al., 2011; Ceolin et al., 2012; Chen et al., 2014; Fukushima et al., 2020). The pharmacological selectivity of PMP was established in analyses of neuronal AMPA, NMDA, and kainate receptor function in cultured neuron and acute brain slice preparations (Hanada et al., 2011; Ceolin et al., 2012; Chen et al., 2014; Barygin, 2016) and in recordings from recombinant expressed iGluRs (Fukushima et al., 2020). The binding site for PMP on AMPARs was localized to key subunit domains that transduce conformational changes in the agonist-binding domains (ABDs) to the channel pore, thereby driving the gating transition from a closed to open state (Yelshanskaya et al., 2016). This binding pocket is also the site of action of other AMPAR NAMs such as GYKI-53655 and CP-465,022 (Lazzaro et al., 2002; Balannik et al., 2005; Hanada et al., 2011; Yelshanskaya et al., 2016), which are thought to inhibit receptor activation by restricting conformational changes underlying channel gating (Balannik et al., 2005).

We tested the hypothesis that PMP inhibits KARs in addition to AMPARs because the structure of PMP in complex with the GluA2 AMPA receptor subunit revealed that most of the residues that form the binding pocket are conserved in the GluK4 and GluK5 KAR subunits (Yelshanskaya et al., 2016). Moreover, a previous study that tested PMP inhibition of recombinant KARs focused solely on homomeric GluK2 receptors (Fukushima et al., 2020). Here, we report that PMP acts as a NAM of heteromeric KARs that incorporate the GluK5 subunit and that inhibition occurs in the same concentration range as AMPA receptors. Two populations of neuronal KARs were also inhibited by PMP, which diverges in part from data reported previously (Ceolin et al., 2012). GluK5 mRNA is expressed throughout the CNS (Watanabe-Iida et al., 2016; Selvakumar et al., 2021), and neuronal KARs are known to incorporate this subunit (Contractor et al., 2003; Vernon and Swanson, 2017), suggesting that a majority of KARs in the brain will be inhibited at therapeutic doses of PMP. We conclude that PMP inhibits both recombinant and neuronal KARs and therefore is not a selective AMPAR NAM. Thus, antiseizure and adverse effects of PMP in patients could arise from differential or tandem inhibition of AMPARs and KARs.

Materials and Methods

Cell culture and transfection. Plasmid DNAs containing the coding sequence for human KAR subunits GluK1–1b (catalog #NM_000830.4), GluK2a (catalog #NM_021956.4), GluK3a (catalog #NM_000831.3), GluK5 (catalog #NM_002088.4), mouse auxiliary protein Neto1 (catalog #NP_659195.3), rat auxiliary protein Neto2 (catalog #NM_001107417.3), and rat AMPA receptor subunit GluA4(i) (flip variant, catalog #NM_017263.2) were transiently expressed in HEK293-T/17 cells [American Type Culture Collection (ATCC) Global Bioresource Center] for use in voltage-clamp recordings. The human GluK2a isoform was used as a template to generate the GluK2(N557D) mutant, and the human GluK5 plasmid was used to generate GluK5 (D540N). Mutations were made using a PCR-based approach and confirmed by sequencing of the open reading frames by the Northwestern University Sanger Sequencing Facility. HEK293-T/17 cells were cultured in DMEM (Corning Cellgro), supplemented with 10% heat-inactivated fetal bovine serum (GeminiBio), and 0.5% penicillin/streptomycin (Corning Cellgro) at 37°C with 5% CO_2. HEK293-T/17 cells were transfected with TransIT-LT1 (Mirus Bio) according to the protocol of the manufacturer. Receptor plasmid DNAs were cotransfected with an enhanced green fluorescent protein (EGFP) and the transfection ratio was 1:6 for EGFP and GluK1; 1:3:0.5 for GluK1, GluK5, and EGFP; 1:3:0.5 for GluK1, Neto1 or Neto2, and EGFP; and 1:3:3:1 for GluK1, GluK5, Neto2, and EGFP cDNAs, respectively. Those ratios were applied similarly for GluK2 or GluK3 containing receptors.

DRG dissection and acute cell isolation. All animals used in these studies were treated according to protocols approved by the Institutional Animal Care and Use Committee of Northwestern University, which were consistent with standards of care established by the *Guide for the Care and Use of Animals*, eighth edition, published by the National Institutes of Health in 2011. Dorsal root ganglia (DRGs) were collected from neonatal male and female C57BL/6 mice (postnatal day 1–8), and DRG neurons were isolated as described previously (Vernon and Swanson, 2017). In brief, animals were anesthetized with isoflurane and decapitated. Lumbar DRGs were collected and digested at 37°C in 1 mg/ml collagenase A/D (Roche) and 0.4 mg/ml activated papain (Roche). DRGs were plated to poly-L-lysine-coated glass coverslips in DMEM (Corning Cellgro) containing 10% fetal bovine serum (GeminiBio) and 0.5% penicillin/streptomycin (Corning Cellgro).

Slice preparation. For mossy fiber EPSC recordings, transverse horizontal brain slices (350 µm) were prepared from 2- to 4-week-old male and female C57BL/6 mice with Leica VT1200S vibratome (Leica Biosystems). Animals were anesthetized and decapitated. The brain was rapidly removed under ice-cold oxygenated sucrose-slicing ACSF containing 85 mM NaCl, 2.5 mM KCl, 1.25 mM NaH_2PO_4, 25 mM $NaHCO_3$, 25 mM glucose, 75 mM sucrose, 10 µM DL-APV, 100 µM kynurenate, 0.5 mM Na L-ascorbate, 0.5 mM $CaCl_2$, and 4 mM $MgCl_2$, equilibrated with 95%O_2/5%CO_2. Slices were incubated at 28°C for 30 min and slowly exchanged from oxygenated sucrose-ACSF for oxygenated ACSF solution containing 125 mM NaCl, 2.4 mM KCl, 1.2 mM NaH_2PO_4, 25 mM $NaHCO_3$, 25 mM glucose, 10 µM DL-APV, 100 µM kynurenate, 0.5 mM Na L-ascorbate, 1 mM $CaCl_2$, and 2 mM $MgCl_2$.

Electrophysiology. Glutamate-evoked currents were recorded from transfected HEK293-T/17 cells and acutely isolated DRG neurons in whole-cell voltage clamp. Recordings were performed 1–3 d after transfection or between 4 and 10 h after isolation of DRG neurons. The external solution contained the following (in mM): 150 NaCl, 2.8 KCl, 2 $CaCl_2$, 1 $MgCl_2$, 10 glucose, and 10 m HEPES (pH adjusted to 7.3 with NaOH). The internal solution used in recordings from transfected cells was composed of the following (in mM): 110 CsF, 30 CsCl, 10 Cs-HEPES, 5 EGTA, 4 M NaCl, and 0.5 $CaCl_2$ (pH adjusted to 7.3 with CsOH). For recordings from DRG neurons, the internal solution contained the following (in mM): 95 CsF, 25 CsCl, 10 Cs-HEPES, 10 Cs-EGTA, 2 Na Cl, 2 Mg-ATP, 10 QX-314, 5 TEA-Cl, and 5 4-AP (pH adjusted to 7.3 with CsOH). Cells were held at −70 mV in voltage clamp with an Axopatch 200B amplifier (Molecular Devices), and glutamate was applied for 100 ms or 1 s as noted with a three-chambered flowpipe attached to a Siskiyou MXPZT-300 solution switcher after lifting the transfected cells from the coverslip into the laminar solution streams. Glutamate-evoked control currents in the absence of PMP were recorded before and after wash-out of PMP from the external solution. Control glutamate concentrations were 30 mM glutamate for GluK3-containing KARs and 10 mM for other receptor combinations. Data were analyzed with Clampfit version 11.0.3 (Molecular Devices).

Recordings from mouse brain slices were conducted at least 2 h after slice preparation. Individual slices were transferred to a recording chamber, continuously perfused with oxygenated ACSF containing 2 mM $CaCl_2$ and 1 mM $MgCl_2$ at 30°C. Whole-cell voltage-clamp recordings were performed from pyramidal neurons in the hippocampal CA3 area using a MultiClamp 700B patch-clamp amplifier (Molecular Devices). CSF internal solution was composed of the following (in mM): 95 CsF, 25 CsCl, 10 Cs-HEPES, 10 Cs-EGTA, 2 NaCl, 2 Mg-ATP, 10 QX-314, and 5 TEA-Cl, 5 4-AP (pH adjusted to 7.3 with CsOH). Mossy fiber

EPSCs were evoked by electrical stimuli generated by an 310 Accupulser (World Precision Instruments). Stimulation electrodes filled with ACSF were positioned in the stratum lucidum. Mossy fiber EPSCs were evoked in the presence of picrotoxin (50 μM) and D-AP5 (50 μM) at a frequency of 1 Hz. $EPSC_{KAR}$ amplitudes were measured 20 ms after the peak of the compound synaptic current in the presence of 0.5 μM NBQX. Trains of EPSCs also were evoked with five stimuli at 100 Hz every 20 s; amplitudes of $EPSC_{KAR}$ were measured 100 ms after the final peak current.

Chemicals. All chemicals except D-AP5 (Hello Bio), DL-AP5 (Hello Bio), picrotoxin (Ascent Scientific), GYKI-53655 (Abcam), and perampanel (Cayman Chemical) were purchased from MilliporeSigma. Perampanel was dissolved in DMSO. The highest concentration of DMSO used in the recordings was 0.3%.

Experimental design and statistical analysis. A target number of recordings for each group was specified; the final numbers varied because of imposition of criteria such as maximal rise time of currents. In some cases, additional data were collected because variation in measured parameters was unexpectedly large or because imposition of criteria reduced the recordings in a group to an unacceptably low number. Summary data are expressed as mean and SD, and confidence intervals are shown in Table 1. Inhibition-response curves were fit to normalized data with the equation $Y = 100/(1 + (IC_{50}/X)\ ^n_H)$, where n_H is the Hill slope, with constrained plateaus at 100 (no inhibition) and 0 (complete inhibition), consistent with our observation that PMP fully eliminated currents in those KAR combinations where it was possible to measure this parameter. Model fitting and statistical tests were performed in GraphPad Prism 9 software. Best-fit curves to the inhibition-response data were compared using an extra sum-of-squares *F* test in GraphPad. Mossy fiber $EPSC_{KAR}$ data were analyzed by one-way ANOVA followed by Dunnett's multiple comparisons test (1 Hz data) or an unpaired *t* test (100 Hz data).

Table 1. IC_{50} Values for PMP inhibition of KARs

Receptor	IC_{50} mean (μM) (SD)	Confidence interval (μM)	*p* Value
GluK1	19 ± 5.3	13–33	
GluK2	26 ± 9.8	17–56	
GluK3	41 ± 5.7	34–56	
GluK1/GluK5	2.8 ± 0.32	2.2–3.5	<0.0001[a]
GluK2/GluK5	0.85 ± 0.09	0.69–1.0	<0.0001[a]
GluK3/GluK5	14 ± 7.5	7.3–37	0.03[a]
GluK1/Neto1	11 ± 4.1	6.9–23	0.13[a]
GluK1/Neto2	19 ± 4.3	13–29	0.94[a]
GluK2/Neto1	5.4 ± 0.94	3.9–7.6	<0.0001[a]
GluK2/Neto2	5.8 ± 0.84	4.4–7.7	<0.0001[a]
GluK1/GluK5/Neto2	0.99 ± 0.15	0.73–1.3	<0.0001[b]
GluK2/GluK5/Neto1	0.69 ± 0.16	0.45–1.1	0.001[b]
GluK2(N557D)	2.8 ± 0.32	2.2–3.5	<0.0001[c]
GluK2(N557D)/GluK5	1.1 ± 0.28	0.72–1.8	0.19[c]
GluK2/GluK5(D540N)	3.0 ± 0.43	2.3–4.0	<0.0001[c]
GluA4(i)	0.56 ± 0.12	0.36–0.85	0.51[d]
DRG neurons	11 ± 1.0	9.4–13	
Mossy fiber $EPSC_{KAR}$	2.9 ± 0.76	1.9–4.9	

Statistical comparisons between IC_{50} values derived from best fits to the inhibition-response data were made pairwise using the extra sum-of-squares *F* test.
[a]Heteromeric receptors compared against their homomeric counterparts.
[b]Neto-containing heteromeric receptors compared against their Neto-less counterparts.
[c]Mutant receptors compared against their wild-type counterparts.
[d]GluA4(i) AMPA receptors compared against GluK2/GluK5/Neto1 KARs.

Results

Structural basis for iGluR selectivity

We initially sought to understand the molecular basis of PMP selectivity for AMPA receptors. The PMP binding site on GluA2 AMPAR subunits is positioned between the clamshell-like ABDs and transmembrane (TM) helices that form the channel pore (Fig. 1*A*; Yelshanskaya et al., 2016; Narangoda et al., 2019; Stenum-Berg et al., 2019). Each subunit in a tetrameric AMPAR contains a PMP binding pocket, which is formed by residues in the pre-M1 linker and M3 and M4 TM helices (Fig. 1*A*,*B*; Yelshanskaya et al., 2016). The sequence alignment shown in Figure 1*C* illustrates putative interacting residues identified in the x-ray crystal structure (blue circles) and in molecular dynamics (MD) simulations (purple circles) in two domains (Yelshanskaya et al., 2016; Narangoda et al., 2019). Although the primary sequences of GluA2 and the KAR subunits GluK1–5 are highly conserved in these regions, notable exceptions occur within the set of PMP binding residues that likely underlie NAM activity on AMPARs. Binding site residues in M3 are not shown because they are identical between AMPAR and KAR subunits. The principal KAR subunits GluK1–3 diverge from GluA2 at binding site residues Ser510, Lys511, and Asp519 in the pre-M1 domain and Ser788 in M4 (positions numbered as per the mature GluA2 subunit; analogous residues in KAR subunits are numbered according to their full-length position in Fig. 1). The GluK3 KAR subunit differs from GluA2 and all four other KAR subunits at Gly513 and Asn791. Notably, the high-affinity KAR subunits GluK4 and GluK5 differ from GluK1–3 but are identical to GluA2 at two critical residues, Lys511 and Asp519 (Fig. 1*C*, blue boxes in the alignment; Yelshanskaya et al., 2016; Narangoda et al., 2019; Stenum-Berg et al., 2019), raising the possibility that these two subunits confer PMP sensitivity to heteromeric KAR subunits.

PMP actions on recombinant KARs

We tested the hypothesis that PMP inhibits KARs in voltage-clamp recordings from recombinant homomeric and heteromeric KARs expressed in HEK293-T/17 cells (Fig. 2). Glutamate was rapidly applied to receptor-expressing cells in the absence and presence of PMP (0.03–30 μM; Fig. 2*A*). The amplitudes of currents gated by homomeric KARs composed of either GluK1, GluK2, or GluK3 subunits were modestly reduced by a high concentration of PMP (10 μM); Fig. 2*A*), which is consistent with an earlier study in which PMP failed to inhibit homomeric GluK2 receptors in patch-clamp recordings (Fukushima et al., 2020). The same concentration of PMP inhibited heteromeric GluK1/GluK5 and GluK2/GluK5 KARs to a much greater extent than their homomeric counterparts. GluK3/GluK5 KARs current amplitudes, on the other hand, appeared only slightly more reduced on average than homomeric GluK3 KARs (Fig. 2*A*). We measured PMP inhibition of each receptor combination at concentrations ranging from 30 nM to 30 μM and fit the data with logistic curves to determine IC_{50} values (Fig. 2*B*). Homomeric KARs were poorly fit as a result of only partial inhibition at the highest concentration tested. These data revealed that incorporation of GluK5 subunits decreased the IC_{50} for GluK1 and GluK2 KARs but had only a modest effect on GluK3 KARs (IC_{50} values on KARs composed of the indicated subunits; GluK1, 19 μM; GluK1/GluK5, 2.8 μM; GluK2, 26 μM; GluK2/GluK5, 0.85 μM; GluK3, 41 μM; GluK3/GluK5, 14 μM; Table 1). Hill slopes ranged from 0.71 to 1.4 with the exception of GluK3/GluK5, which had a shallow slope of 0.42 and was not inhibited fully at 30 μM. GluK1/GluK5 and GluK2/GluK5 KARs were inhibited in a concentration range similar to that of AMPA receptors (Hanada et al., 2011; Fukushima et al., 2020) as the inhibition-response curve for GluA4(i) AMPA receptors also demonstrates (IC_{50} of 0.56 μM, Hill slope of 0.80; Fig. 2*B*). Collectively, these results are

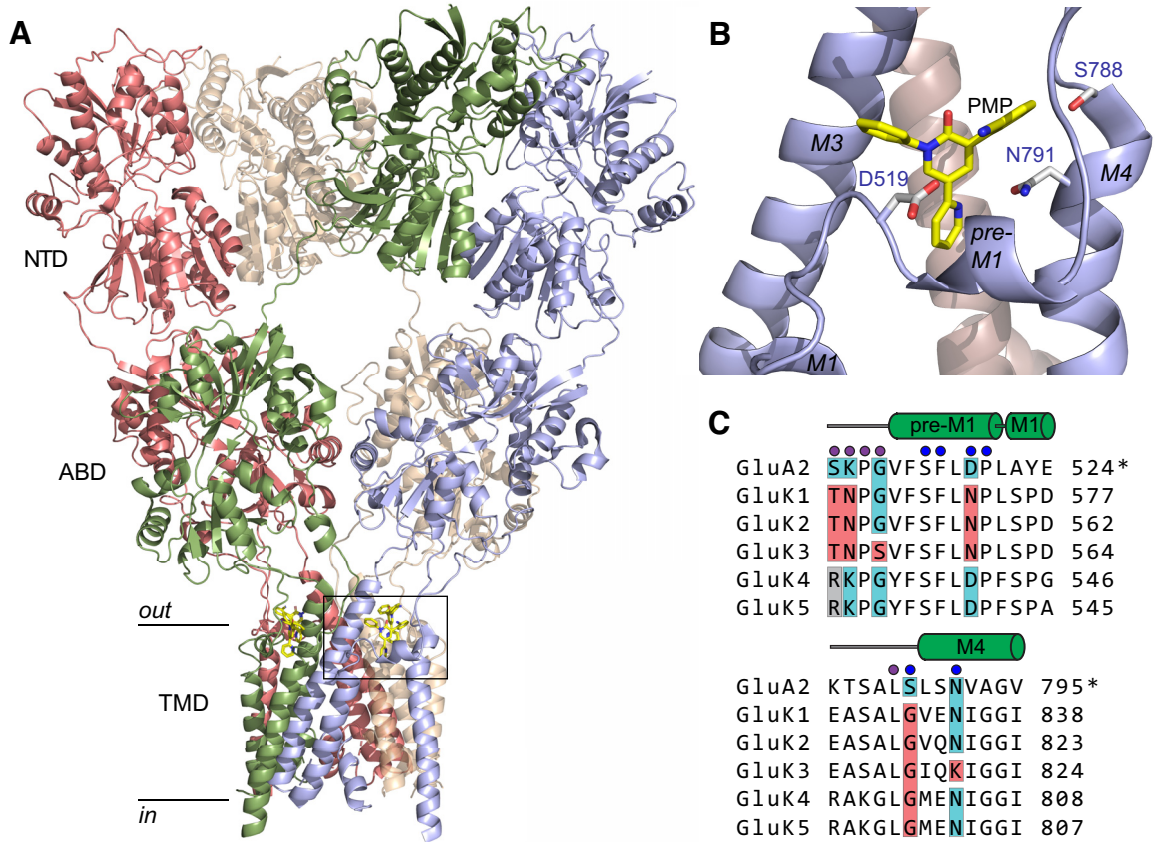

Figure 1. PMP binding site and sequence comparison. ***A***, Tetrameric structure of the homomeric GluA2 AMPAR docked with PMP (c:5L1F; Yelshanskaya et al., 2016). Subunit proteins consist of N-terminal domains (NTDs), ABDs, and transmembrane domains (TMD). The intracellular carboxy-terminal was not resolved. PMP was localized to a binding pocket between the linker region and the external segments of TMDs (boxed region). ***B***, The PMP binding site in homomeric GluA2 AMPAR (boxed region in ***A***). Interacting residues that differ in one or more KAR subunit are labeled and are D519 in the pre-M1 linker, S788 in the pre-M4 linker, and N791 in the M4 transmembrane helix. ***C***, Sequence alignment between PMP-binding domains in GluA2 and the analogous segments in each KAR subunit. Blue circles identify residues likely to interact with PMP in the x-ray crystal structure (Yelshanskaya et al., 2016); purple circles show additional residues that interact with PMP in multiple poses from MD simulations (Narangoda et al., 2019) or inferred from mutagenesis experiments (Stenum-Berg et al., 2019). GluA2 numbering is the mature protein (indicated by the "*"), whereas KAR subunits are numbered as per the full sequence. The M3 domain is omitted because the primary sequence is identical in AMPAR and KAR subunits. Binding site residues that diverge between subunits are shaded. GluA2 and identical residues in KAR subunits are shaded in blue. Red shading shows positional divergence in one or more KAR subunits. The gray boxes at S510 (GluA2 numbering) in GluK4 and GluK5 show divergence from both GluA2 and GluK1–3 KAR subunits.

consistent with a strong subunit-dependency of PMP NAM activity on KARs.

Neto1 and Neto2 auxiliary proteins alter KAR function and pharmacology in a variety of ways dependent on the precise subunit composition of the receptors (Copits et al., 2011; Straub et al., 2011a,b; Fisher and Mott, 2013) and are constituents of neuronal KARs (Straub et al., 2011a; Wyeth et al., 2014; Vernon and Swanson, 2017). Residues near the putative PMP binding site in homomeric and heteromeric KARs appear critical for modulation of channel kinetics by Neto2 (Griffith and Swanson, 2015). Accordingly, we tested the hypothesis that incorporation of Neto auxiliary proteins alters PMP NAM activity on homomeric and heteromeric KARs in recordings from GluK1/Neto1, GluK2/Neto1, GluK1/Neto2, and GluK2/Neto2 KARs (Fig. 3*A*) and a pair of heteromeric receptor/auxiliary protein combinations predicted to be similar in composition to KARs expressed by sensory neurons in DRGs (GluK1/GluK5/Neto2; Mulle et al., 2000; Vernon and Swanson, 2017) and at CA3 pyramidal cell mossy fiber synapses (GluK2/GluK5/Neto1; Mulle et al., 2000; Fernandes et al., 2009; Straub et al., 2011b; Fig. 3*A*).

These data revealed an unexpected divergence in the effect of Neto assembly with GluK1-containing receptors and those with GluK2 subunits. As shown in the representative traces in Figure 3*A* (at 10 μM PMP), neither Neto1 nor Neto2 altered NAM inhibition of homomeric GluK1 KARs (IC_{50} values, GluK1, 19 μM; GluK1/Neto1, 11 μM; GluK1/Neto2, 19 μM; Fig. 3*B*), whereas both auxiliary proteins modestly increased sensitivity of homomeric GluK2 KARs (IC_{50} values, GluK2, ~26 μM; GluK2/Neto1, 5.4 μM; GluK2/Neto2, 5.8 μM). Neither Neto1 nor Neto2 enhanced the PMP sensitivity beyond that conferred by GluK5 in heteromeric receptors that mimic those in DRG neurons (GluK1/GluK5/Neto2; IC_{50} = 0.99 μM) or hippocampal CA3 pyramidal neurons (GluK2/GluK5/Neto1; IC_{50} = 0.69 μM; Fig. 3*A*,*B*).

We next tested the relevance of a key pre-M1 residue to differential PMP actions on GluK2 and GluK5 subunits. Aspartate 519 (GluA2 numbering; Asn557 in GluK2 and Asp540 in GluK5; Yelshanskaya et al., 2016) is essential for inhibition of AMPA receptors by the NAM CP-465 022 (Balannik et al., 2005), which overlaps with PMP in its binding site on GluA2 subunits (Yelshanskaya et al., 2016). GluK2 KAR subunits mutated to include an aspartate at this position in place of the encoded asparagine were inhibited by CP-465 022, unlike wild-type homomeric GluK2 receptors (Balannik et al., 2005). To determine whether the same residue plays a role in PMP inhibition of KARs, we recorded from receptors composed of GluK2 (N557D) and GluK5(D540N) subunits. Homomeric GluK2 (N557D) KARs were substantially inhibited by 10 μM PMP

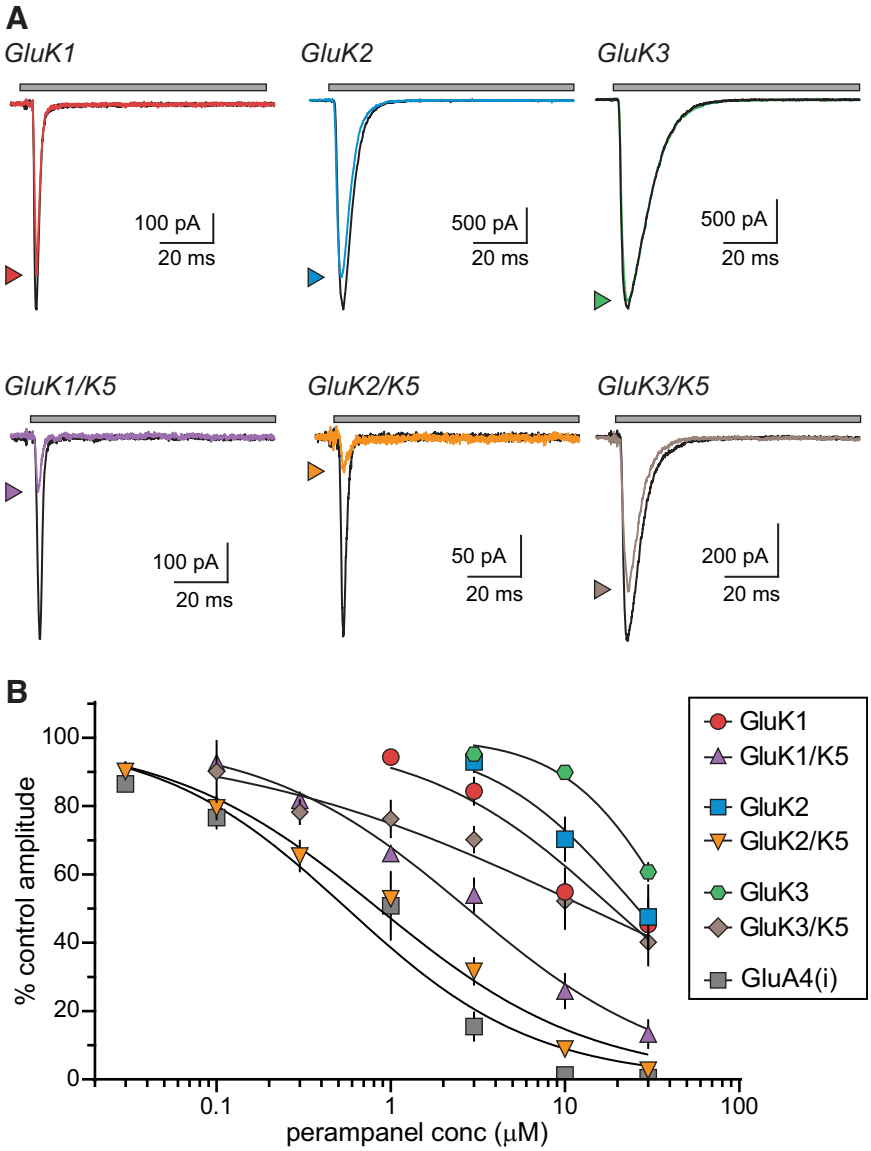

Figure 2. PMP inhibition of recombinant homomeric and heteromeric KARs. ***A***, Representative currents from recombinant homomeric and heteromeric KARs. Currents were evoked by glutamate for 100 ms either alone (black lines) or in the presence of PMP (10 μM, colored lines). Top, The gray bar denotes glutamate application. The current amplitudes of heteromeric GluK1/GluK5 and GluK2/GluK5 KARs are markedly decreased by PMP compared with those of homomeric GluK1 or GluK2 KARs. PMP did not inhibit either GluK3 or GluK3/GluK5 KARs to a substantial degree. ***B***, Normalized mean amplitudes of currents evoked from recombinant homomeric and heteromeric KARs at a range of PMP concentrations were best fit with logistic curves with variable IC_{50} and Hill slopes. Homomeric GluA4(i) AMPARs are shown for comparison to demonstrate that GluK2/GluK5 KARs are inhibited in the same concentration range as AMPARs. IC_{50} values, 95% confidence intervals, and statistical analyses are shown in Table 1.

(Fig. 4*A*,*B*) to a much greater degree than wild-type GluK2 KARs (Fig. 2*A*), suggesting that the asparagine at this position in GluK2 is principally responsible for preventing inhibition of homomeric GluK2 receptors. Heteromeric GluK2(N557D)/GluK5 were inhibited by PMP to roughly the same extent as wild-type GluK2/GluK5 receptors (Fig. 4*A*,*B*). We also recorded from heteromeric GluK2/GluK5(D540N) receptors to test the importance of the analogous residue in GluK5 in generating PMP sensitivity. These receptors exhibited an intermediate degree of PMP inhibition between homomeric GluK2 and heteromeric GluK2/GluK5 receptors (Fig. 4*A*,*B*). IC_{50} values for these receptors were the following: GluK2(N557D), 2.8 μM; GluK2(N557D)/GluK5, 1.1 μM; and GluK2/GluK5(D540N), 3.0 μM (Fig. 4*B*, Table 1). These data implicate Asp557 as a principal determinant that occludes PMP inhibition of homomeric GluK2 receptors. Conversely, mutation of Asp540 in GluK5 does not abrogate PMP activity, and therefore other residues contribute to NAM binding to KAR receptors containing this subunit.

PMP inhibition of neuronal KARs

Our data suggest that neuronal KARs containing the GluK5 subunit will be sensitive to inhibition by PMP. We tested this hypothesis by examining the effect of PMP on well-characterized neuronal receptors expressed by nociceptive DRG neurons and those localized to hippocampal mossy fiber–CA3 pyramidal neuron synapses; KARs in both populations contain GluK5 and either Neto2 (DRGs) or Neto1 (mossy fibers; Mulle et al., 2000; Contractor et al., 2003; Straub et al., 2011a; Vernon and Swanson, 2017).

The sensitivity of DRG KARs to PMP was determined in voltage-clamp recordings of glutamate-evoked currents from small- to medium-diameter neurons acutely isolated from lumbar DRGs of neonatal mice. iGluR currents in DRG neurons at this age arise solely from KARs (Huettner, 1990; Mulle et al., 2000), allowing a straightforward analysis of PMP NAM activity on neuronal KARs. PMP (30 μM) inhibited glutamate-evoked currents in DRG neurons, as predicted from the results of recombinant receptors, whereas GYKI-53655 exhibited very little NAM activity at the same concentration (Fig. 5*A*). The peak amplitude of glutamate-evoked currents was reduced by 77.6 ± 4.6% by PMP and 10.2 ± 4.4% by GYKI-53655 (both at 30 μM, $n = 12$ and 10, respectively). Fitting of data over a range of concentrations yielded an estimated IC_{50} of 11.2 μM for PMP (Fig. 5*B*, Table 1).

We examined whether PMP decreases the KAR-mediated EPSCs ($EPSC_{KAR}$) at mossy fiber synapses. Postsynaptic KAR currents were elicited with 1 Hz stimuli, as described previously (Ito et al., 2004; Fernandes et al., 2009). AMPA receptors were inhibited selectively with a low concentration of NBQX (0.5 μM) in the extracellular solution (Perrais et al., 2009). We chose this approach rather than targeting AMPARs with GYKI-53655 because the binding site for this NAM overlaps that of PMP (Hanada et al., 2011; Yelshanskaya et al., 2016). KAR current amplitudes were measured at 20 ms after the peak of the EPSCs during 1 Hz stimulation to avoid any residual contribution by AMPARs (Fig. 6*A*). As shown in the representative traces, PMP (30 μM) almost eliminated the $EPSC_{KAR}$, whereas currents in the presence of GYKI-53655 ran down to an equivalent degree as the vehicle control (DMSO) condition (Fig. 6*A*,*B*). PMP inhibition also was observed when we evoked mossy fiber EPSCs with a train of five stimuli at

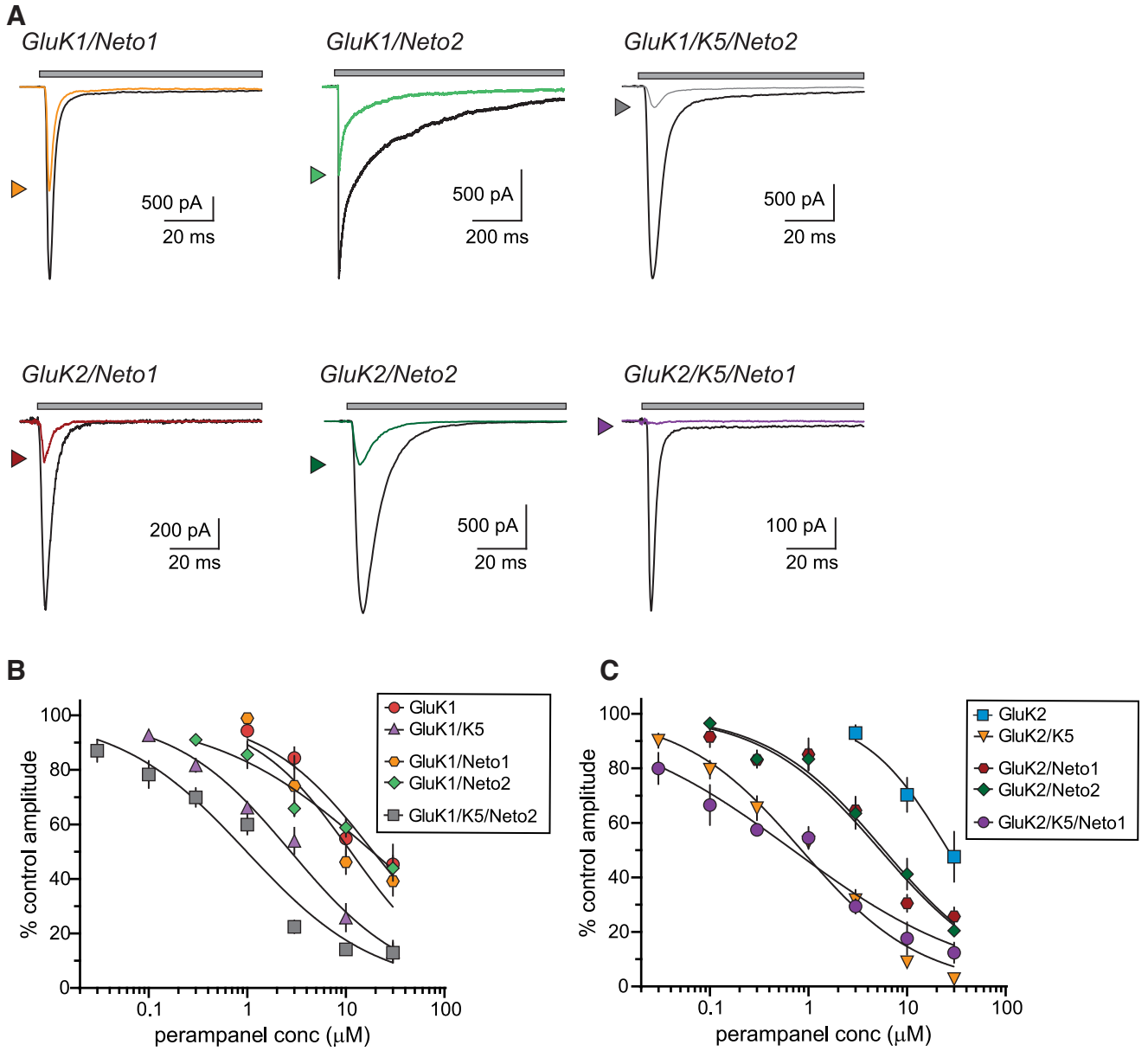

Figure 3. PMP inhibition of KARs containing Neto1 or Neto2 auxiliary subunits. ***A***, Representative currents from recombinant homomeric and heteromeric KARs containing either Neto1 or Neto2 auxiliary proteins (GluK1, top; GluK2, bottom). Currents were evoked by glutamate either alone (black lines) or in the presence of PMP (10 μM, colored lines) for either 1 s (GluK1/Neto2) or 100 ms (others). Top, The gray bar denotes glutamate application. GluK2/Neto1 and GluK2/Neto2 KARs were inhibited to a greater extent than GluK1 receptors with either Neto1 or Neto2. ***B***, Normalized mean amplitudes of currents evoked from GluK1 and GluK1/GluK5 KARs with and without Neto proteins at a range of PMP concentrations were best fit with logistic curves with variable IC_{50} and Hill slopes. The data and fitted curves for GluK1 and GluK1/GluK5 KARs are identical to those in Figure 2 and are shown for the sake of comparison. IC_{50} values, 95% confidence intervals, and statistical analyses are shown in Table 1. ***C***, Normalized mean amplitudes of currents evoked from GluK2 and GluK2/GluK5 KARs with and without Neto proteins at a range of PMP concentrations were best fit with logistic curves with variable IC_{50} and Hill slopes. The data and fitted curves for GluK2 and GluK2/GluK5 KARs are identical to those in Figure 2 and are shown for the sake of comparison. IC_{50} values, 95% confidence intervals, and statistical analyses are shown in Table 1.

100 Hz in the absence of NBQX (Fig. 6*A*); the slow decay of the currents after the last stimuli is predominantly carried by synaptic KARs and is minimally altered by GYKI-53655. $EPSC_{KAR}$ at 1 Hz stimulation were reduced in a concentration-dependent manner by 1, 10, and 30 μM PMP (Fig. 6*B*). $EPSC_{KAR}$ commonly exhibits a slow run down in amplitude of ~20% over 10 min of recording, which is apparent in the DMSO control and GYKI-53655 time courses shown in Figure 6*B*. The concentration dependence of inhibition for currents evoked by 1 Hz stimulation in the presence of NBQX (Fig. 6*C*) yielded an estimated IC_{50} value of 2.9 μM (Table 1), which is comparable to the values observed with the recombinant GluK5-containing heteromeric receptors. KAR synaptic currents evoked by five stimuli at 100 Hz were eliminated by PMP but only partially reduced by GYKI-53655 (each at 30 μM) in the absence of NBQX (Fig. 6*C*). These data demonstrate that PMP inhibits KARs at mossy fiber–CA3 pyramidal cell synapses.

Discussion

We demonstrate here that perampanel inhibits KARs in addition to AMPARs and that NAM activity on KARs requires either the GluK5 subunit or one of the Neto auxiliary proteins as a channel constituent. The broad expression of GluK5 mRNA in neurons

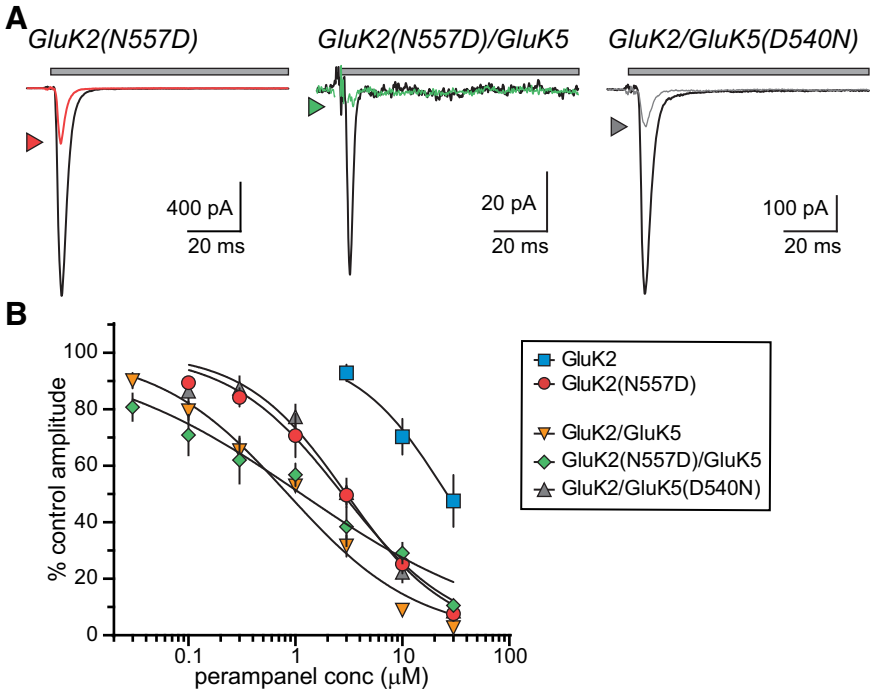

Figure 4. The role of a key amino acid in PMP inhibition of KARs. ***A***, Representative currents from GluK2 and GluK2/GluK5 KARs containing mutations that swap the respective amino acids at a key binding site determinant (N557 in GluK2, D540 in GluK5). Currents were evoked by glutamate (10 mM for 100 ms) either alone (black lines) or in the presence of PMP (10 μM, colored lines) for 100 ms. Top, The gray bar denotes glutamate application. ***B***, Normalized mean amplitudes of currents evoked from GluK2(N557D), GluK2(N557D)/GluK5, and GluK2/GluK5(D540N) at a range of PMP concentrations were best fit with logistic curves with variable IC_{50} and Hill slopes. The data and fitted curves for GluK2 and GluK2/GluK5 KARs are identical to those in Figure 2 and are shown for the sake of comparison. IC_{50} values, 95% confidence intervals, and statistical analyses are shown in Table 1. Reciprocal swaps at this site increased sensitivity of homomeric GluK2 KARs to PMP attenuated but did not eliminate PMP inhibition of GluK5(D540N)-containing KARs.

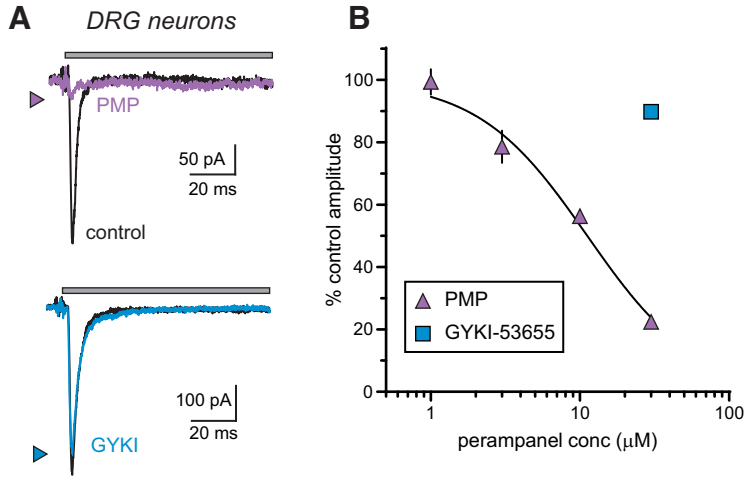

Figure 5. Neuronal KARs expressed by nociceptive DRG neurons are inhibited by PMP. ***A***, Representative glutamate-evoked currents recorded from acutely isolated DRG neurons in control conditions (black lines) or those in the presence of 30 μM PMP (purple line) or 30 μM GYKI-53655 (blue line). Top, The gray bar shows the timing of glutamate application (100 ms). Thirty micromolar PMP almost eliminates the current, whereas the same concentration of GYKI-53655 shows little effect. ***B***, Mean amplitudes of currents evoked from DRG neurons normalized to DMSO (0.3%) controls at a range of PMP concentrations were best fit with a logistic curve with variable IC_{50} and Hill slopes. Inhibition-response curves of the percent inhibition of KARs in the DRG neurons at a range of PMP concentrations. The IC_{50} value and 95% confidence interval are shown in Table 1.

throughout the CNS suggested that most KARs will be susceptible to PMP inhibition (Bahn et al., 1994), and indeed that proved to be the case for KARs localized to hippocampal synapses (Castillo et al., 1997; Contractor et al., 2003) and in lumbar DRG neurons (Huettner, 1990; Vernon and Swanson, 2017). PMP is efficacious for treatment of focal and generalized tonic-clonic seizures; however, a black-box warning for suicidal ideation and psychiatric disturbances is associated with PMP because of severe adverse effects in some patients (Rugg-Gunn, 2014; Zhuo et al., 2017; Villanueva et al., 2022). Our findings raise the possibility that therapeutic and adverse effects of PMP arise differentially from inhibition of either AMPA or kainate receptors or because signaling by both types of receptors is suppressed.

Our data show that AMPARs are not the sole molecular target for PMP. Recombinant KARs were insensitive to PMP in a previous study based on patch-clamp recordings from homomeric GluK2 KARs (Fukushima et al., 2020), and we similarly observed that homomeric GluK2 KARs were relatively insensitive to PMP. However, KARs composed solely of GluK2 subunits (or solely of GluK1 or GluK3) are unlikely to be highly represented in the CNS neurons (Selvakumar et al., 2021). The GluK5 subunit is widely expressed across the CNS (Bahn et al., 1994; Selvakumar et al., 2021), and a variety of receptor populations exhibit more complex stoichiometries in functional and molecular studies (Mulle et al., 2000; Christensen et al., 2004; Fernandes et al., 2009; Selvakumar et al., 2021). PMP inhibition of heteromeric KARs containing GluK5 subunits or Neto auxiliary proteins in the same concentration range as AMPA receptors suggests that the drug will act as a nonselective AMPA and kainate receptor NAM throughout the nervous system.

PMP interacts with discrete residues in AMPARs that are highly conserved in KAR subunits (Yelshanskaya et al., 2016; Narangoda et al., 2019). Our initial mapping of the binding site residues that diverge between GluK2 and GluK5 centered on Asn557 of GluK2, which is known to control differential inhibition of AMPA and kainate receptors by CP-465 022 (Balannik et al., 2005). Similarly, GluK2 gained PMP sensitivity when Asn557 was mutated to the aspartate found in GluK5 and AMPAR subunits. PMP binding within the GluA2 pocket appears to be promiscuous based on the variety of stable poses observed in simulations (Narangoda et al., 2019), which might underlie our observation that mutation of the analogous Asp540 in GluK5 to an asparagine did not completely eliminate PMP inhibition. Molecular docking of PMP into a GluK2 cryo-EM structure (PDB:5KUF) and comparison with GluK2(N557D) did not yield

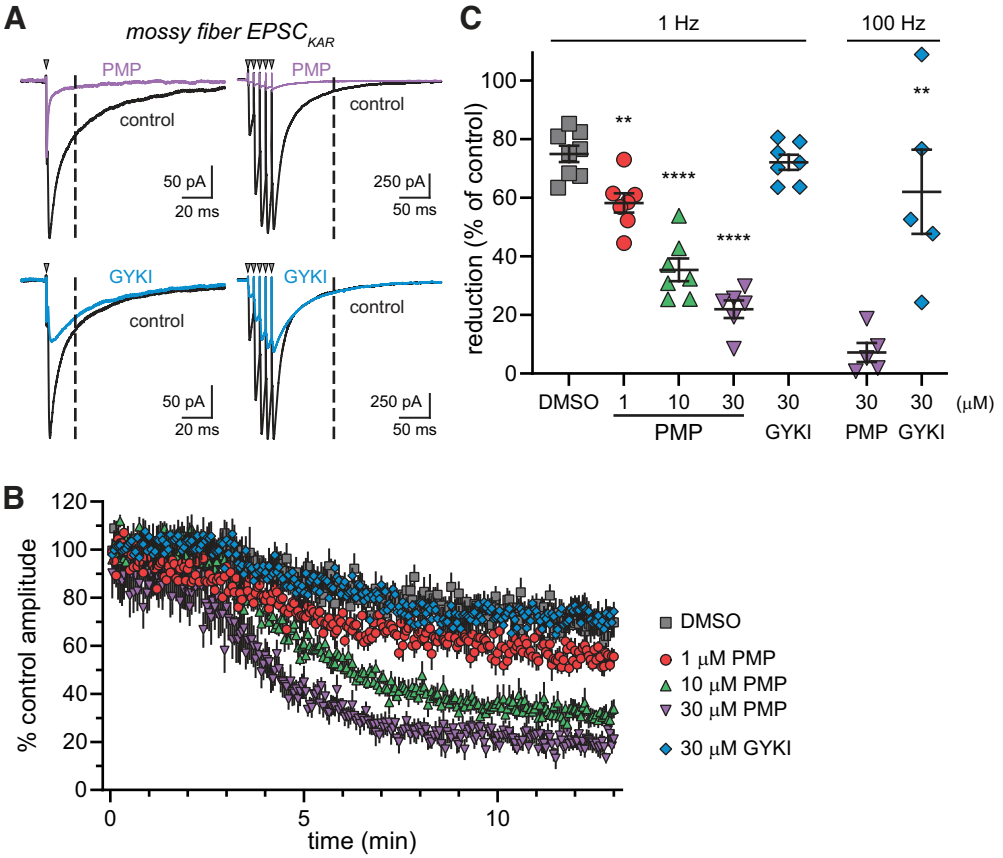

Figure 6. KARs at mossy fiber CA3 pyramidal cell synapses are inhibited by PMP. ***A***, Representative $EPSC_{KAR}$ recorded at mossy fiber synapses in control conditions (black lines) or those in the presence of 30 μM PMP (purple line) or 30 μM GYKI-53655 (blue line). Synaptic currents were evoked by stimulation of the stratum lucidum at 1 Hz (left) or with 5 stimuli at 100 Hz (right). NBQX (0.5 μM) was present during $EPSC_{KAR}$ recording at 1 Hz but not 100 Hz. The amplitude of $EPSC_{KAR}$s were measured at 20 ms after the peak of the mixed AMPAR/KAR EPSC during 1 Hz stimulation or 100 ms after the last peak current following 100 Hz stimulation (dashed lines). PMP inhibited both AMPA and kainate receptor components, whereas GYKI-53655 only had an effect on AMPA receptors. ***B***, time course changes of the percentage amplitude of $EPSC_{KAR}$ in response to PMP, GYKI-53655, or DMSO application. Current amplitudes were normalized to the mean amplitudes of first 20 $EPSC_{KAR}$. DMSO was applied as a control for run down of the currents. The time course of $EPSC_{KAR}$ amplitudes in the presence of DMSO and GYKI-53655 overlap, whereas PMP produced concentration-dependent inhibition. ***C***, Summary data showing the mean, SE, and data from individual recordings for the percentage inhibition of $EPSC_{KAR}$ by PMP after 10 min of application. Significance indicated as $^{**}p < 0.01$ and $^{****}p < 0.0001$ compared with DMSO-treated group (1 Hz) or the amplitudes of $EPSC_{KAR}$ in the presence of GYKI-53655 compared with PMP (100 Hz).

mechanistic insight into how this residue acts as a determinant of PMP inhibition (data not shown). We also do not understand how Neto proteins alter the binding domain to favor PMP interactions for GluK2-containing receptors, even in the absence of GluK5. The cryo-EM structures of GluK2 and Neto2 suggest that the auxiliary protein is unlikely to directly contact gating linkers (He et al., 2021); however, alteration of the M3-S2 linker changes the efficacy of Neto2 modulation (Griffith and Swanson, 2015), perhaps indirectly as a result of Neto2 interactions with adjacent membrane and ligand-binding domains.

PMP inhibited central and peripheral neuronal KARs. Hippocampal mossy fiber–CA3 pyramidal $EPSC_{KAR}$ typically is differentiated from AMPA receptors in *ex vivo* recordings using the AMPA receptor-selective NAM GYKI-53655 or the AMPA/kainate receptor NAM GYKI-52466. However, these compounds and PMP have overlapping binding sites on AMPA receptors (Barygin, 2016; Yelshanskaya et al., 2016), which is likely the case for KARs as well (Balannik et al., 2005). We circumvented the confounding actions of overlapping NAMs by instead isolating the $EPSC_{KAR}$ with two approaches. First, we measured a KAR-enriched synaptic current in the presence of a low concentration of the competitive AMPA receptor antagonist NBQX and by measuring the effect of PMP 20 ms after peak current amplitude, as was done previously (Perrais et al., 2009). Second, we measured the $EPSC_{KAR}$ after a brief, high-frequency train of stimulation at a time point when the AMPA receptor component decayed to baseline. The experiments definitively show that mossy fiber $EPSC_{KAR}$ is inhibited by low micromolar concentrations of PMP but not GYKI-53655 (Fig. 6; Paternain et al., 1995; Castillo et al., 1997). Our observations diverge, however, from a study in which the KAR component of mossy fiber EPSPs was insensitive to PMP (Ceolin et al., 2012). We speculate that the different experiment outcomes can be reconciled because KAR-mediated EPSPs recorded previously were isolated pharmacologically using a high concentration of GYKI-52466 that competed for binding to synaptic KARs and thereby occluded further inhibition by PMP.

PMP also inhibited KARs in nociceptive DRG neurons. Acutely isolated, small-diameter neonatal DRG and trigeminal ganglia neurons are the only known cell type in which glutamate-evoked currents arise exclusively from KARs (Huettner, 1990; Sahara et al., 1997), making these neurons of particular use in validating the action of PMP as an inhibitor. PMP reduced glutamate-evoked currents in neonatal DRG neurons with an IC_{50} of ~11 μM (Fig. 5), whereas GYKI-53655 was ineffective, again consistent with the expression of GluK1/GluK5 and Neto2 in a subset of DRG and trigeminal neurons (Huettner, 1990;

Sahara et al., 1997; Mulle et al., 2000; Vernon and Swanson, 2017). KARs have been implicated in nocifensive behaviors in preclinical pharmacological and genetic models of neuropathic and inflammatory pain (Simmons et al., 1998; Dominguez et al., 2005; Ko et al., 2005; Qiu et al., 2011; Bhangoo and Swanson, 2013), migraine (Filla et al., 2002; Andreou et al., 2009, 2015), and itch-induced scratching (Descalzi et al., 2013). Moreover, antagonists with mixed AMPA and GluK1-containing KARs showed efficacy for alleviation of pain in Phase I clinical trials before drug development programs were terminated (Gilron et al., 2000; Sang et al., 2004). Thus, PMP antagonism of KARs on sensory neurons or nociceptive pathways could in part underlie the analgesic actions of the drug and potential efficacy in pain management (Khangura et al., 2017; Hara et al., 2020) or in alleviation of itch (Haruta-Tsukamoto et al., 2020).

The relevance of KAR inhibition to PMP antiseizure actions remains to be elucidated. KAR activation with chemoconvulsants that include the eponymous agonist kainic acid potently induces seizures in rodents, and the resultant structural and pathologic alterations reproduce many hallmark features of human temporal lobe epilepsy (TLE; Ben-Ari, 1985; Ben-Ari and Cossart, 2000; Rusina et al., 2021). Further dissection of the contribution of a specific type of KARs—those containing GluK1 subunits—have produced contradictory results, with antiepileptiform and antiseizure efficacy observed with both GluK1-selective agonists (Khalilov et al., 2002) and KAR antagonists (Smolders et al., 2002; Pinheiro et al., 2013) in a variety of *in vitro* and *in vivo* rodent models. Activation of hippocampal GluK2-containing KARs has been implicated in seizure induction (Mulle et al., 1998; Yu et al., 2016) and in maintenance of chronic seizure states (Epsztein et al., 2005; Peret et al., 2014) in chemoconvulsant models of TLE. These and other studies have provided strong evidence that KARs play complex and model-dependent roles in the seizures elicited in some (but not all) chemoconvulsant and electrical stimulation-induced epileptiform behavior in rodents (Henley et al., 2021; Mulle and Crépel, 2021).

The abundant preclinical observations linking KAR signaling and rodent seizure models have not yet led to a framework for understanding their importance to human epilepsies. In large part this knowledge gap exists because KAR antagonists also inhibit AMPARs, with the exception of modestly selective GluK1-targeting antagonists (Larsen and Bunch, 2011), which have not been tested for antiseizure efficacy in randomized trials. It is likely, however, that overactivation of human KARs causes a pathology like that observed in rodent TLE models because consumption of toxic levels of the high-affinity KAR agonist domoic acid in contaminated mussels causes acute seizures, cognitive deficits, gastrointestinal symptoms, and even death (Perl et al., 1990; Teitelbaum et al., 1990). One individual developed focal seizures with secondary generalization and an extensive loss of hippocampal CA3 pyramidal neurons (Cendes et al., 1995). More recently, severe intractable epilepsies were reported in children with a *de novo* gain-of-function variant in the *GRIK2* gene, which encodes GluK2 subunits, suggesting that aberrant KAR signaling can cause profound disruption of CNS development (Stolz et al., 2021). The potential benefits to epilepsy patients of inhibiting KARs, however, remain unknown, with one possible exception. Topiramate, a regulatory approved ASD with a variety of molecular targets, inhibits GluK1-preferring agonist-evoked currents and seizures through indirect mechanisms that have not been resolved (Gryder and Rogawski, 2003; Kaminski et al., 2004). It remains to be determined whether topiramate and PMP share a molecular basis for their antiseizure efficacy.

In conclusion, we demonstrate that PMP inhibits KARs containing the GluK5 subunit or Neto auxiliary proteins and is therefore not a selective AMPA receptor NAM. Our results raise the possibility that KAR inhibition could underlie some aspects of antiseizure or adverse effects associated with PMP use for epilepsy. Drug discovery aimed at more selective NAMs that discriminate between AMPARs and KARs could yield drugs with an improved therapeutic profile.

References

Andreou AP, Holland PR, Goadsby PJ (2009) Activation of iGluR5 kainate receptors inhibits neurogenic dural vasodilatation in an animal model of trigeminovascular activation. Br J Pharmacol 157:464–473.

Andreou AP, Holland PR, Lasalandra MP, Goadsby PJ (2015) Modulation of nociceptive dural input to the trigeminocervical complex through GluK1 kainate receptors. Pain 156:439–450.

Bahn S, Volk B, Wisden W (1994) Kainate receptor gene expression in the developing rat brain. J Neurosci 14:5525–5547.

Balannik V, Menniti FS, Paternain AV, Lerma J, Stern-Bach Y (2005) Molecular mechanism of AMPA receptor noncompetitive antagonism. Neuron 48:279–288.

Barygin OI (2016) Inhibition of calcium-permeable and calcium-impermeable AMPA receptors by perampanel in rat brain neurons. Neurosci Lett 633:146–151.

Ben-Ari Y (1985) Limbic seizure and brain damage produced by kainic acid: mechanisms and relevance to human temporal lobe epilepsy. Neuroscience 14:375–403.

Ben-Ari Y, Cossart R (2000) Kainate, a double agent that generates seizures: two decades of progress. Trends Neurosci 23:580–587.

Bhangoo SK, Swanson GT (2013) Kainate receptor signaling in pain pathways. Mol Pharmacol 83:307–315.

Castillo PE, Malenka RC, Nicoll RA (1997) Kainate receptors mediate a slow postsynaptic current in hippocampal CA3 neurons. Nature 388:182–186.

Cendes F, Andermann F, Carpenter S, Zatorre RJ, Cashman NR (1995) Temporal lobe epilepsy caused by domoic acid intoxication: evidence for glutamate receptor-mediated excitotoxicity in humans. Ann Neurol 37:123–126.

Ceolin L, Bortolotto ZA, Bannister N, Collingridge GL, Lodge D, Volianskis A (2012) A novel anti-epileptic agent, perampanel, selectively inhibits AMPA receptor-mediated synaptic transmission in the hippocampus. Neurochem Int 61:517–522.

Chen CY, Matt L, Hell JW, Rogawski MA (2014) Perampanel inhibition of AMPA receptor currents in cultured hippocampal neurons. PLoS One 9: e108021.

Chen Z, Brodie MJ, Liew D, Kwan P (2018) Treatment outcomes in patients with newly diagnosed epilepsy treated with established and new antiepileptic drugs: a 30-year longitudinal cohort study. JAMA Neurol 75:279–286.

Christensen JK, Paternain AV, Selak S, Ahring PK, Lerma J (2004) A mosaic of functional kainate receptors in hippocampal interneurons. J Neurosci 24:8986–8993.

Contractor A, Sailer AW, Darstein M, Maron C, Xu J, Swanson GT, Heinemann SF (2003) Loss of kainate receptor-mediated heterosynaptic facilitation of mossy-fiber synapses in KA2$^{-/-}$ mice. J Neurosci 23:422–429.

Copits BA, Robbins JS, Frausto S, Swanson GT (2011) Synaptic targeting and functional modulation of GluK1 kainate receptors by the auxiliary neuropilin and tolloid-like (NETO) proteins. J Neurosci 31:7334–7340.

Descalzi G, Chen T, Koga K, Li XY, Yamada K, Zhuo M (2013) Cortical GluK1 kainate receptors modulate scratching in adult mice. J Neurochem 126:636–650.

Dominguez E, et al. (2005) Two prodrugs of potent and selective GluR5 kainate receptor antagonists actives in three animal models of pain. J Med Chem 48:4200–4203.

Epsztein J, Represa A, Jorquera I, Ben-Ari Y, Crépel V (2005) Recurrent mossy fibers establish aberrant kainate receptor-operated synapses on granule cells from epileptic rats. J Neurosci 25:8229–8239.

Fernandes HB, Catches JS, Petralia RS, Copits BA, Xu J, Russell TA, Swanson GT, Contractor A (2009) High-affinity kainate receptor subunits are

necessary for ionotropic but not metabotropic signaling. Neuron 63:818–829.
Filla SA, et al. (2002) Ethyl (3S,4aR,6S,8aR)-6-(4-ethoxycar- bonylimidazol-1-ylmethyl)decahydroiso-quinoline-3-carboxylic ester: a prodrug of a GluR5 kainate receptor antagonist active in two animal models of acute migraine. J Med Chem 45:4383–4386.
Fisher JL, Mott DD (2013) Modulation of homomeric and heteromeric kainate receptors by the auxiliary subunit Neto1. J Physiol 591:4711–4724.
Fukushima K, Hatanaka K, Sagane K, Ido K (2020) Inhibitory effect of antiseizure medications on ionotropic glutamate receptors: special focus on AMPA receptor subunits. Epilepsy Res 167:106452.
Gilron I, Max MB, Lee G, Booher SL, Sang CN, Chappell AS, Dionne RA (2000) Effects of the 2-amino-3-hydroxy-5-methyl-4-isoxazole-propionic acid/kainate antagonist LY293558 on spontaneous and evoked postoperative pain. Clin Pharmacol Ther 68:320–327.
Golyala A, Kwan P (2017) Drug development for refractory epilepsy: the past 25 years and beyond. Seizure 44:147–156.
Griffith TN, Swanson GT (2015) Identification of critical functional determinants of kainate receptor modulation by auxiliary protein Neto2. J Physiol 593:4815–4833.
Gryder DS, Rogawski MA (2003) Selective antagonism of GluR5 kainate-receptor-mediated synaptic currents by topiramate in rat basolateral amygdala neurons. J Neurosci 23:7069–7074.
Hanada T, Hashizume Y, Tokuhara N, Takenaka O, Kohmura N, Ogasawara A, Hatakeyama S, Ohgoh M, Ueno M, Nishizawa Y (2011) Perampanel: a novel, orally active, noncompetitive AMPA-receptor antagonist that reduces seizure activity in rodent models of epilepsy. Epilepsia 52:1331–1340.
Hara K, Haranishi Y, Terada T (2020) Intrathecally administered perampanel alleviates neuropathic and inflammatory pain in rats. Eur J Pharmacol 872:172949.
Haruta-Tsukamoto A, Miyahara Y, Funahashi H, Nishimori T, Ishida Y (2020) Perampanel attenuates scratching behavior induced by acute or chronic pruritus in mice. Biochem Biophys Res Commun 533:1102–1108.
He L, Sun J, Gao Y, Li B, Wang Y, Dong Y, An W, Li H, Yang B, Ge Y, Zhang XC, Shi YS, Zhao Y (2021) Kainate receptor modulation by NETO2. Nature 599:325–329.
Henley JM, Nair JD, Seager R, Yucel BP, Woodhall G, Henley BS, Talandyte K, Needs HI, Wilkinson KA (2021) Kainate and AMPA receptors in epilepsy: cell biology, signalling pathways and possible crosstalk. Neuropharmacology 195:108569.
Huettner JE (1990) Glutamate receptor channels in rat DRG neurons: activation by kainate and quisqualate and blockade of desensitization by Con A. Neuron 5:255–266.
Ito K, Contractor A, Swanson GT (2004) Attenuated plasticity of postsynaptic kainate receptors in hippocampal CA3 pyramidal neurons. J Neurosci 24:6228–6236.
Kaminski RM, Banerjee M, Rogawski MA (2004) Topiramate selectively protects against seizures induced by ATPA, a GluR5 kainate receptor agonist. Neuropharmacology 46:1097–1104.
Khalilov I, Hirsch J, Cossart R, Ben-Ari Y (2002) Paradoxical anti-epileptic effects of a GluR5 agonist of kainate receptors. J Neurophysiol 88:523–527.
Khangura RK, Bali A, Kaur G, Singh N, Jaggi AS (2017) Neuropathic pain attenuating effects of perampanel in an experimental model of chronic constriction injury in rats. Biomed Pharmacother 94:557–563.
Ko S, Zhao MG, Toyoda H, Qiu CS, Zhuo M (2005) Altered behavioral responses to noxious stimuli and fear in glutamate receptor 5 (GluR5)- or GluR6-deficient mice. J Neurosci 25:977–984.
Larsen AM, Bunch L (2011) Medicinal chemistry of competitive kainate receptor antagonists. ACS Chem Neurosci 2:60–74.
Lazzaro JT, Paternain AV, Lerma J, Chenard BL, Ewing FE, Huang J, Welch WM, Ganong AH, Menniti FS (2002) Functional characterization of CP-465,022, a selective, noncompetitive AMPA receptor antagonist. Neuropharmacology 42:143–153.
Mulle C, Crépel V (2021) Regulation and dysregulation of neuronal circuits by KARs. Neuropharmacology 197:108699.
Mulle C, Sailer A, Pérez-Otaño I, Dickinson-Anson H, Castillo PE, Bureau I, Maron C, Gage FH, Mann JR, Bettler B, Heinemann SF (1998) Altered synaptic physiology and reduced susceptibility to kainate-induced seizures in GluR6-deficient mice. Nature 392:601–605.
Mulle C, Sailer A, Swanson GT, Brana C, O'Gorman S, Bettler B, Heinemann SF (2000) Subunit composition of kainate receptors in hippocampal interneurons. Neuron 28:475–484.
Narangoda C, Sakipov SN, Kurnikova MG (2019) AMPA receptor noncompetitive inhibitors occupy a promiscuous binding site. ACS Chem Neurosci 10:4511–4521.
Paternain AV, Morales M, Lerma J (1995) Selective antagonism of AMPA receptors unmasks kainate receptor-mediated responses in hippocampal neurons. Neuron 14:185–189.
Patsalos PN (2015) The clinical pharmacology profile of the new antiepileptic drug perampanel: a novel noncompetitive AMPA receptor antagonist. Epilepsia 56:12–27.
Peret A, Christie LA, Ouedraogo DW, Gorlewicz A, Epsztein J, Mulle C, Crépel V (2014) Contribution of aberrant GluK2-containing kainate receptors to chronic seizures in temporal lobe epilepsy. Cell Rep 8:347–354.
Perl TM, Bédard L, Kosatsky T, Hockin JC, Todd EC, Remis RS (1990) An outbreak of toxic encephalopathy caused by eating mussels contaminated with domoic acid. N Engl J Med 322:1775–1780.
Perrais D, Pinheiro PS, Jane DE, Mulle C (2009) Antagonism of recombinant and native GluK3-containing kainate receptors. Neuropharmacology 56:131–140.
Pinheiro PS, Lanore F, Veran J, Artinian J, Blanchet C, Crépel V, Perrais D, Mulle C (2013) Selective block of postsynaptic kainate receptors reveals their function at hippocampal mossy fiber synapses. Cereb Cortex 23:323–331.
Qiu CS, Lash-Van Wyhe L, Sasaki M, Sakai R, Swanson GT, Gereau RW 4th (2011) Antinociceptive effects of MSVIII-19, a functional antagonist of the GluK1 kainate receptor. Pain 152:1052–1060.
Rogawski MA (2011) Revisiting AMPA receptors as an antiepileptic drug target. Epilepsy Curr 11:56–63.
Rogawski MA (2013) AMPA receptors as a molecular target in epilepsy therapy. Acta Neurol Scand 127:9–18.
Rugg-Gunn F (2014) Adverse effects and safety profile of perampanel: a review of pooled data. Epilepsia 55 Suppl 1:13–15.
Rusina E, Bernard C, Williamson A (2021) The kainic acid models of temporal lobe epilepsy. eNeuro 8:ENEURO.0337-20.2021–0320.2021.
Sahara Y, Noro N, Iida Y, Soma K, Nakamura Y (1997) Glutamate receptor subunits GluR5 and KA-2 are coexpressed in rat trigeminal ganglion neurons. J Neurosci 17:6611–6620.
Sang CN, Ramadan NM, Wallihan RG, Chappell AS, Freitag FG, Smith TR, Silberstein SD, Johnson KW, Phebus LA, Bleakman D, Ornstein PL, Arnold B, Tepper SJ, Vandenhende F (2004) LY293558, a novel AMPA/GluR5 antagonist, is efficacious and well-tolerated in acute migraine. Cephalalgia 24:596–602.
Selvakumar P, Lee J, Khanra N, He C, Munguba H, Kiese L, Broichhagen J, Reiner A, Levitz J, Meyerson JR (2021) Structural and compositional diversity in the kainate receptor family. Cell Rep 37:109891.
Sills GJ, Rogawski MA (2020) Mechanisms of action of currently used antiseizure drugs. Neuropharmacology 168:107966.
Simmons RM, Li DL, Hoo KH, Deverill M, Ornstein PL, Iyengar S (1998) Kainate GluR5 receptor subtype mediates the nociceptive response to formalin in the rat. Neuropharmacology 37:25–36.
Smolders I, Bortolotto ZA, Clarke VR, Warre R, Khan GM, O'Neill MJ, Ornstein PL, Bleakman D, Ogden A, Weiss B, Stables JP, Ho KH, Ebinger G, Collingridge GL, Lodge D, Michotte Y (2002) Antagonists of GLU(K5)-containing kainate receptors prevent pilocarpine-induced limbic seizures. Nat Neurosci 5:796–804.
Stenum-Berg C, Musgaard M, Chavez-Abiega S, Thisted CL, Barrella L, Biggin PC, Kristensen AS (2019) Mutational analysis and modeling of negative allosteric modulator binding sites in AMPA receptors. Mol Pharmacol 96:835–850.
Stolz JR, et al. (2021) Clustered mutations in the GRIK2 kainate receptor subunit gene underlie diverse neurodevelopmental disorders. Am J Hum Genet 108:1692–1709.
Straub C, Hunt DL, Yamasaki M, Kim KS, Watanabe M, Castillo PE, Tomita S (2011a) Distinct functions of kainate receptors in the brain are determined by the auxiliary subunit Neto1. Nat Neurosci 14:866–873.
Straub C, Zhang W, Howe JR (2011b) Neto2 modulation of kainate receptors with different subunit compositions. J Neurosci 31:8078–8082.
Teitelbaum JS, Zatorre RJ, Carpenter S, Gendron D, Evans AC, Gjedde A, Cashman NR (1990) Neurologic sequelae of domoic acid intoxication

due to the ingestion of contaminated mussels. N Engl J Med 322:1781–1787.

Vernon CG, Swanson GT (2017) Neto2 assembles with kainate receptors in DRG neurons during development and modulates neurite outgrowth in adult sensory neurons. J Neurosci 37:3352–3363.

Villanueva V, D'Souza W, Goji H, Kim DW, Liguori C, McMurray R, Najm I, Santamarina E, Steinhoff BJ, Vlasov P, Wu T, Trinka E (2022) PERMIT study: a global pooled analysis study of the effectiveness and tolerability of perampanel in routine clinical practice. J Neurol 269:1957–1977.

Watanabe-Iida I, Konno K, Akashi K, Abe M, Natsume R, Watanabe M, Sakimura K (2016) Determination of kainate receptor subunit ratios in mouse brain using novel chimeric protein standards. J Neurochem 136:295–305.

Wyeth MS, Pelkey KA, Petralia RS, Salter MW, McInnes RR, McBain CJ (2014) Neto auxiliary protein interactions regulate kainate and NMDA receptor subunit localization at mossy fiber-CA3 pyramidal cell synapses. J Neurosci 34:622–628.

Yelshanskaya MV, Singh AK, Sampson JM, Narangoda C, Kurnikova M, Sobolevsky AI (2016) Structural bases of noncompetitive inhibition of AMPA-subtype ionotropic glutamate receptors by antiepileptic drugs. Neuron 91:1305–1315.

Yu LM, Polygalov D, Wintzer ME, Chiang MC, McHugh TJ (2016) CA3 synaptic silencing attenuates kainic acid-induced seizures and hippocampal network oscillations. eNeuro 3:ENEURO.0003-16.2016.

Zaccara G, Giovannelli F, Cincotta M, Iudice A (2013) AMPA receptor inhibitors for the treatment of epilepsy: the role of perampanel. Expert Rev Neurother 13:647–655.

Zhuo C, Jiang R, Li G, Shao M, Chen C, Chen G, Tian H, Li J, Xue R, Jiang D (2017) Efficacy and tolerability of second and third generation anti-epileptic drugs in refractory epilepsy: a network meta-analysis. Sci Rep 7:2535.